2001 International Conference on Indium Phosphide and Related Materials
Conference Proceedings
13th IPRM 14-18, May 2001 Nara, Japan

InP/InGaAsP WAFER-BONDED VERTICALLY COUPLED X-CROSSING MULTIPLE CHANNEL OPTICAL ADD-DROP MULTIPLEXER

M. A. Raburn, B. Liu[a)], Y. Okuno, and J. E. Bowers

Electrical and Computer Engineering Department
University of California, Santa Barbara, CA 93106
a) Calient Networks, 25 Castillian Drive, Goleta, California 93117
This work is supported by the DARPA center MOST.

Abstract

A vertically coupled InP/InGaAsP crossed waveguide optical add-drop multiplexer (OADM) has been realized through the use of wafer bonding. Designed for signals in the 1550-nm range, this novel device requires only a single epitaxial growth and illustrates the use of vertical optical interconnects for the three-dimensional routing of optical signals. To our knowledge, it is also one of the first optical vertically coupled devices with no horizontally coupled counterpart.

I. Introduction

Optical Add-Drop Multiplexers (OADMs) are key channel routing components in Wavelength-Division Multiplexed (WDM) systems. OADM implementation methods include fiber or polymer gratings with circulators [(1)], arrayed waveguides [(2)], and cascaded unbalanced Mach-Zehnder structures [(3)]. InP/InGaAsP OADMs [(4)] are of particular interest because monolithic integration of other optoelectronic devices onto the same chip is possible. Vertical coupling enables the creation of simpler, shorter devices than equivalent horizontally coupled structures, and also allows laterally separated inputs and outputs for ease of coupling to fibers when wafer bonding is employed [(5)].

In this letter, a simple multi-channel OADM is proposed and demonstrated. The device consists of straight waveguides that cross to form X's. One "in/through" top waveguide is vertically coupled to, and crossed at an angle of 0.3° with, four parallel "add/drop" bottom waveguides (Figure 1). Only one growth was required for the structure because waveguides were etched on both surfaces of the epitaxial material. The OADM operation is based on coherent coupling of light between the top waveguide and a bottom waveguide, which will only take place when their effective refractive indices are nearly identical. The different widths of the four add/drop waveguides thus correspond to different channels, as the effective indices are functions of both wavelength and waveguide width.

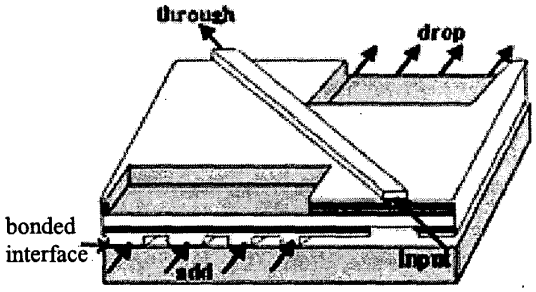

Fig. 1. Layout of the OADM.

II. Device Fabrication And Structure

Vertically coupled waveguides that cross to form long, narrow X's were fabricated. One wafer was grown using MOCVD (Metal-Organic Chemical Vapor Deposition). On a (001) InP substrate, a 0.2-μm InGaAs etch stop, 0.8-μm InP layer, 15-nm InGaAsP etch stop, 0.2-μm InP cladding layer, 1-μm InGaAsP (λ_g=1.066μm) guiding layer, 1.5-μm InP cladding and support layer, 0.22-μm InGaAsP (λ_g=1.359μm) guiding layer, 0.4-μm InP cladding layer, 15-nm InGaAsP etch stop, and 0.8-μm InP layer were grown.

The bottom waveguides were fabricated first because the bonding and substrate removal steps in effect reverse the epitaxial growth order. The device fabrication began with the deposition of SiN, standard photolithography, and CF_4 plasma etching to form a SiN etch mask. Wet etching of the top 0.8-μm InP layer ($HCl:H_2O$=2:1) defined the position of the bottom layer waveguides. Another set of SiN, photolithography, and wet etching steps ($HCl:H_2O$=2:1, $H_2SO_4:H_2O_2:H_2O$=1:1:10) removed the etch stop layer,

the 0.4-μm InP layer and the 0.22-μm bottom guiding layer in certain regions (Figure 1). These layers will induce unwanted coupling of light from the top waveguide to the slab mode of the bottom waveguide guiding layer if allowed to remain. After thorough cleaning, the sample was bonded at 630°C in a nitrogen atmosphere for 50 minutes to a new, blank InP wafer cleaved to the same size. The substrate and the 0.2-μm etch stop layer of the grown wafer were removed via wet etching. The backside of the new InP wafer was then polished to aide in the subsequent infrared (IR) photolithography, which defined the top layer waveguides while alignment with the bottom-level pattern was maintained. Processing of the top waveguides was the same as that for the bottom except $CH_4/H_2/Ar$ reactive ion etching was used instead of wet etching. Lastly, the sample was cleaved.

III. Device Design

The finished OADMs were 60μm wide and 1.2cm long. Each device has one top in/through waveguide of width 3μm and four parallel bottom add/drop waveguides of width 2, 3, 4, and 5μm, separated laterally by 10μm for coupling into lensed fibers (Figure 2). Since growth variations cause changes in the fraction of light coupled, crossing angles between the top waveguide and the four bottom waveguides ranging from 0.2° to 0.45° were used. The x-crossing arrangement allowed by the bonding also provides lateral separation of the top waveguide from the four bottom waveguides. Support regions were placed 10μm away from all waveguides to ensure that neither deformation of the structure nor unwanted coupling to the supports would occur.

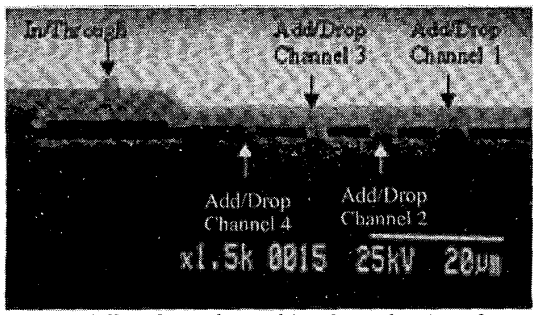

Fig. 2. SEM of sample resulting from cleaving of output facet, including in/through waveguide and four add/drop waveguides.

If the difference between the propagation constants of two crossed waveguides is very small, after a given length, light entering one waveguide will couple completely to the other waveguide. Dissimilar indices and dimensions for the top and bottom waveguides were chosen because the difference in material and waveguide dispersion allows complete coupling over a much narrower wavelength range than with identical coupled waveguides. Away from the center wavelength, the coupling will be very small due to the phase mismatch. The x-crossing geometry reduces coherent coupling of sidelobes as well [4].

The effective index and transfer matrix methods [6,7] were used to calculate the effective refractive indices at different wavelengths, material compositions, and waveguide widths. The material compositions were altered slightly from the previous single channel OADM design [4] because it was found that [8] while the formerly used Henry et al approach [9] gave a satisfactory relationship between bandgap and index of refraction of InGaAsP for smaller bandgaps (1.3μm-1.55μm), the expression derived by Weber [10] provided a better approximation for higher bandgaps (~1.1μm).

This 4-channel OADM does not have a horizontally coupled equivalent, as the waveguides cannot be rearranged or bent in such a manner that they yield an in-plane device with the same capabilities without excessive losses or crosstalk. The dissimilarity between the top and bottom waveguides further complicates any approach to reduce the number of dimensions. Thus, this device illustrates the wonderful flexibility in layout afforded by wafer bonding to form vertically coupled structures.

IV. Results

A tunable semiconductor laser with a polarization controller was used to investigate the behavior of the devices. The bandgaps of the InGaAsP regions of the actual growth (λ_g=1.066μm, λ_g=1.359μm) deviated slightly from that of the desired growth (λ_g=1.068μm, λ_g=1.370μm) needed for room temperature operation. This offset necessitated the heating of the sample to 104.3°C to shift the indices of the material to allow coupling within the range of the tunable laser. The temperature-induced shift in the center wavelengths of the drop channels was 0.39nm/°C.

The center wavelength of the device has a strong dependence on the InGaAsP bandgaps due to the large dispersion difference between the top and bottom waveguides. Increasing the bandgap wavelength of the top waveguide InGaAsP by 1nm decreases the center wavelength of the device by 4.1nm; the ratio of wavelength shifts for the bottom InGaAsP is 2.5:1. The growth variation of InGaAsP bandgaps was 10nm.

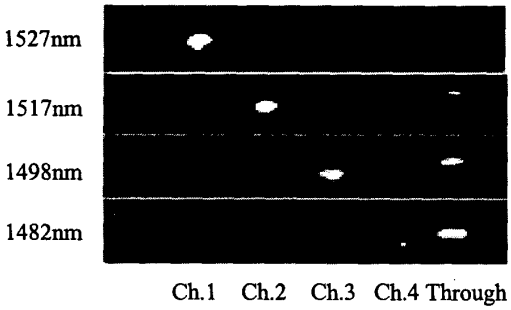

Fig. 3. Output of OADM as captured with IR camera and 80x microscope objective lens.

The near-field output is shown in Figure 3 at the peak wavelength of each channel. The four channels lie at 1482nm, 1498nm, 1517nm, and 1527nm. Figure 4 shows a wavelength scan of the OADM throughput and the first three channels. Unfortunately, the fourth channel was damaged before the data for Figure 4 was taken. The high temperature required for operation of the device aggravated air drafts around the lensed fibers, resulting in noise despite attempts to shield the setup; smoothed data is hence plotted.

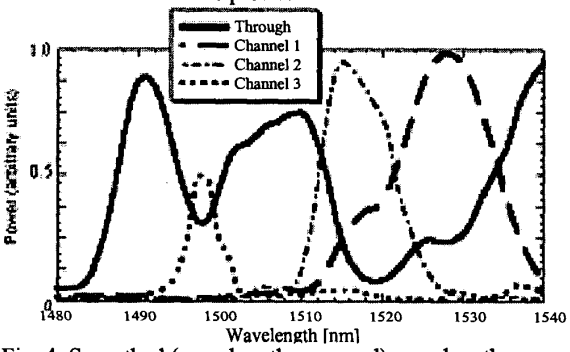

Fig. 4. Smoothed (wavelength averaged) wavelength scan of OADM.

The four bottom waveguide widths were chosen such that the four channels would be close in wavelength yet suffer low crosstalk. Though due to the undesirable growth, this was not the case for channels 1 and 2, the crosstalk between channels 2 and 3 is less than –17dB. Adjusting the waveguide widths for 20nm channel spacing would give a maximum crosstalk of –15dB for all channels. This wide channel spacing indicates suitability for datacom rather than telecom operation. The bandwidth can be reduced by decreasing the crossing angle, decreasing the thickness of InP between the InGaAsP guiding layers (Figure 5), or using guiding materials with more different dispersion characteristics (e.g. InP/InGaAsP bonded to AlGaAs/GaAs).

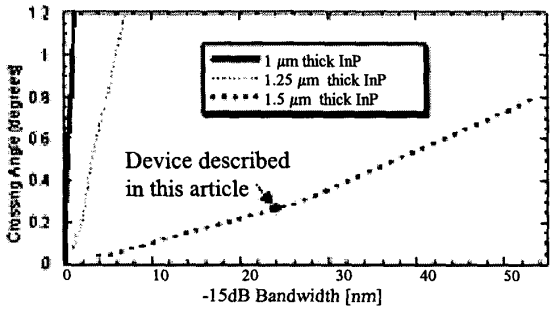

Fig. 5. Theoretical OADM bandwidth as determined by crossing angle, thickness of InP between the two InGaAsP guiding layers.

82% of channel 1, 93% of channel 2, and 65% of channel 3 are dropped. Simulations predict that the maximum intensities of all channels can be made equal by using slightly different crossing angles between the in/through waveguide and each add/drop waveguide. The percentage of power dropped can be increased through fine-tuning the crossing angles as well.

Another property matching theoretical predictions is stronger coupling for TE polarizations. TE and TM coupling wavelengths were found to differ by 200nm. TM-oriented light resulted in a drop channel intensity 11dB less than that for TE light. The polarization sensitivity results from the strong waveguide geometry asymmetry; large material dispersion differences rather than waveguide dispersion differences (e.g. InP/InGaAsP bonded to AlGaAs/GaAs) would allow TE and TM coupling at the same wavelength. An OADM with waveguide parameters adjusted for TM coupling can be cascaded after the OADM described here for polarization-independent coupling as well.

The fiber-to-fiber device loss was 11.3dB. The in/through waveguide loss was 7.7dB/cm using a Fabry-Perot resonance technique [11].

V. Conclusion

A novel InP/InGaAsP vertical coupler OADM is demonstrated. Though the layout is simple, the device cannot be reduced to two dimensions. This illustrates the powerful potential of wafer bonding to fabricate three-dimensional photonic integrated circuits.

Acknowledgement

The authors thank K. Gill and Dr. A. Keating for useful discussions and continuous encouragement.

References

[1] H. Mavoori, S. Jin, R. P. Espindola, and T. A. Strasser, "Enhanced thermal and magnetic actuations for broad-range tuning of fiber Bragg grating-based reconfigurable add-drop devices," *Opt. Lett.*, vol. 24, pp. 714-716, 1999.

[2] C.R. Doerr, L. W. Stulz, J. Gates, M. Cappuzzo, E. Laskowski, L. Gomez, A. Paunescu, A. White, and C. Narayanan, "Arrayed waveguide lens wavelength add-drop in silica," *IEEE Photon. Technol. Lett.*, vol. 11, pp.239-241, 1999.

[3] B. J. Offrein, G. L. Bona, F. Horst, W. M. Salemink, R. Beyeler, and R. Germann, "Wavelength tunable optical add-after-drop filter with flat passband for WDM networks," *IEEE Photon. Technol. Lett.*, vol. 11, pp. 239-241, 1999.

[4] B. Liu, A. Shakouri, P. Abraham, and J. E. Bowers, "Optical Add/Drop Multiplexers Based on X-Crossing Vertical Coupler Filters," *IEEE Photon. Technol. Lett.*, vol. 12, pp.410-412, 2000.

[5] M. Raburn, B. Liu, P. Abraham, and J.E. Bowers, "Double fused InP/InGaAsP vertical coupler beam splitter," *IEEE Photon. Technol. Lett.*, vol. 12, pp.1639-41, 2000.

[6] L. Coldren and S. Corzine, Diode Lasers and Photonic Integrated Circuits, New York: John Wiley & Sons, Inc. 1995.

[7] J. Chilwell and I. Hodgkinson, "Thin-films field-transfer matrix theory of planar multilayer waveguides and reflection from prism-loaded waveguides," *J. Opt. Soc. America A*, vol. 1, pp. 742-753, 1984.

[8] B. Broberg and S. Lindgren, "Refractive index of $In_{1-x}Ga_xAs_yP_{1-y}$ layers and InP in the transparent wavelength region," *Journal of Applied Physics*, vol. 55, pp. 3376-81,1984.

[9] C. H. Henry, L. F. Johnson, R. A. Logan, and D. P. Clarke, "Determination of the refractive index of InGaAsP epitaxial layers by mode line luminescence spectroscopy," *IEEE J. Quantum Electron.*, vol. QE-21, pp. 1887-92, 1985.

[10] J. P. Weber, "Optimization of the Carrier-Induced Effective Index Change in InGaAsP Waveguides—Application to Tunable Bragg Filters," *IEEE J. Quantum. Electron.*, vol. 30, pp. 1801-1816, 1994.

[11] K. H. Park, M. W. Kim, Y. T. Byun, D. Woo, S. H. Kim, and S. S. Choi, "Nondestructive propagation loss and facet reflectance measurements of GaAs/AlGaAs strip-loaded waveguides," *J. Appl. Phys.*, 78(10), 6318-6320, November (1995).